

# Development of Model Predictive Control Algorithm for Managing Deformation of Multilayered Soil Massif under Mass and Heat Transfer

Nataliia Zhukovska<sup>a</sup>, Viktor Moshynskiy<sup>a</sup>, Viktor Zhukovskyy<sup>a</sup>, Andriy Sverstiuk<sup>b</sup> and Oleg Pinchuk<sup>a</sup>

<sup>a</sup> National University of Water and Environmental Engineering, 11 Soborna St., Rivne, 33028, Ukraine

<sup>b</sup> I. Horbachevsky Ternopil National Medical University, 12 Rus'ka St., Ternopil, 46001, Ukraine

## Abstract

The study of soil foundation deformation processes is important in the context of intensive construction development. The stress-strain state of both buildings and the soil foundations on which they are built are interconnected. To ensure the operational reliability of structures, it is necessary to consider the displacement, stress, and strain values of soil arrays and their dynamic behavior. This article focuses on the spatial stress-strain state of a multilayered soil massif, considering the effect of mass and heat transfer during the filtration of salt solutions. The soil massif is shaped like a curved quadrangle, consisting of multiple layers with distinct physical, chemical, and elastic characteristics. One of the layers has a free surface, which is considered fixed. The mathematical model of the problem is based on solid-state mechanics approaches, including deformable body mechanics, porous media, filtration, and mass and heat transfer theory. The model comprises a system of equilibrium equations for soil displacement in Lamé form, considering mass and heat transfer, convective diffusion equations in the presence of mass and heat transfer throughout the studied soil massif, and equations for normal and tangential strains and stresses. The model also accounts for equations of salt solutions filtration under non-isothermal conditions in water-saturated layers, equations of convective heat transfer in the entire field of study, as well as corresponding boundary conditions at the boundaries of the soil massif and ideal contact conjugation conditions for piezometric head, salt concentration, temperature, displacements, and stresses. The model takes into account the dependence of Lamé coefficients and filtration coefficients on salt solution concentration and temperature during construction.

## Keywords 1

Spatial stress-strain state, free surface, mass and heat transfer, filtering multilayer soil mass.

## 1. Introduction

Soil is a heterogeneous environment that naturally consists of multiple layers, such as sand, clay, loam, humus, and chernozem [9]. Previous studies have investigated the processes of filtration, mass and heat transfer, and stress-strain state in soils in the presence of pure water [7]. However, in natural conditions, various saline solutions are also filtered, and the effect of temperature is present. Filtration is slower in clay soil layers and faster in sand, indicating that these factors can affect the stress-strain state of each layer of the soil massif. These processes can also affect the stability of facilities built on such soils and result in unpredictable accidents and significant economic losses. Mathematical and computer modeling can be used to study these processes, with three-dimensional modeling allowing for an adequate description of physical processes in space and the possibility of future analysis [13].

---

CITIT'2023: 1st International Workshop on Computer Information Technologies in Industry 4.0, June 14–16, 2023, Ternopil, Ukraine  
EMAIL: n.a.zhukovska@nuwm.edu.ua (A. 1); v.s.moshynskiy@nuwm.edu.ua (A. 2); v.v.zhukovskyy@nuwm.edu.ua (A. 3), sverstyuk@tdmu.edu.ua (A. 4); o.l.pinchuk@nuwm.edu.ua (A. 5)  
ORCID: 0000-0001-7839-0684 (A. 1); 0000-0002-1661-6809(A. 2), 0000-0002-7088-6930 (A. 3); 0000-0001-8644-0776 (A. 4); 0000-0001-6566-0008 (A. 5)



© 2023 Copyright for this paper by its authors.  
Use permitted under Creative Commons License Attribution 4.0 International (CC BY 4.0).  
CEUR Workshop Proceedings (CEUR-WS.org)

There have been numerous studies conducted on multilayered soils and their deformation behavior. One study [6] proposes a semi-analytical approach for calculating ground movements caused by tunnel construction in multilayered clay soils. Another study [8] employs a three-layer polygon model simulated with the finite element method, exploring the effects of hydraulic conductivity, shear modulus, degree of saturation, molecular diffusion coefficient, and thickness of each layer on multilayered systems. Nonlinear loading of large foundations on multilayered saturated soils was investigated in [5], with their mathematical model revealing that the point of maximum deformation is not necessarily in the center of the foundation, nor does it coincide with the point of maximum load, as discussed in [12]. Spatial deformation processes in multilayered soils involve three displacement values, six normal and tangential strain values, and six normal and tangential stress values. Therefore, the investigation of the stress-strain state of soil environments is of scientific interest, and is the objective of the current study.

## 2. Formulation of the problem

Let us consider the multilayered soil massif with a free surface in the three-dimensional case (see Figure 1). The soil massif is shaped curvilinear quadrangle and occupies the  $\Omega$  area, where  $\Omega = \Omega_{i^*} \cup \Omega_{i^*}$ ,  $\Omega_{i^*} = \bigcup_{i=1}^k \Omega_i$ ,  $\Omega_{i^*} = \bigcup_{i=k+1}^n \Omega_i$ . The number of layers in the soil massif is  $n$ . The layers are numbered from bottom to top. In the area  $\Omega_k$  there is a free surface  $\Gamma_v$  and it is considered stationary. The layers of the soil massif located above  $\Gamma_v$  ( $\Omega_{i^*}$ ), are in the natural state, and below  $\Gamma_v$  ( $\Omega_{i^*}$ ) are water-saturated.

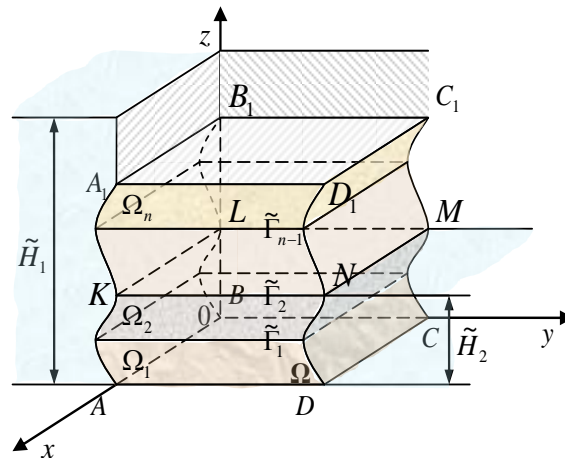


**Figure 1:** The spatial scheme of a multilayered soil massif with a free surface

In the area  $\Omega$  there are processes of stress-strain state, filtration of salts solutions in non-isothermal conditions and heat and mass transfer. Moreover, the processes of filtration of salts solutions and mass transfer occur only in water-saturated areas.

We consider the linear theory of elasticity. The top and bottom of the area  $\Omega$  are impermeable and insulated. The sides of the soil massif are drained. There are water basins with water levels  $\tilde{H}_1$  and  $\tilde{H}_2$  ( $\tilde{H}_1 > \tilde{H}_2$ ) on the sides  $AA_1B_1B$ ,  $B_1BCC_1$  and  $AKND$ ,  $DNMC$  respectively.

Each layer of  $\Omega$  has its own physicochemical and mechanical properties. Elastic parameters and filtration coefficient in water-saturated layers ( $\Omega_{i^*}$ ) depend on the concentration of salts solutions and temperature,  $\lambda_i = \lambda_i(c_{i^*}, T_i)$ ,  $\mu_i = \mu_i(c_{i^*}, T_i)$ ,  $K_i = K_i(c_{i^*}, T_i)$ , and depend on the temperature in the in the natural state soil layers ( $\Omega_{i^*}$ ),  $\lambda_i = \lambda_i(T_{i^*})$ ,  $\mu_i = \mu_i(T_{i^*})$ ,  $K_i = K_i(T_{i^*})$ . Some of the most common salts in nature, such as  $NaCl$  and  $KCl$ , which are extracted for the food industry ( $NaCl$ ) and

used in the agricultural sector (*KCl*), were used as studies in salt solutions. The laws of Darcy, Fick and Fourier are apply in the area  $\Omega$ .

### 3. Mathematical model of the problem

The mathematical model of the spatial stress-strain state problem of multilayered soil massif at the presence the filtration of salts solutions in non-isothermal conditions and mass and heat transfer in the generally accepted designations has the following form [1-3, 7, 10, 11, 14, 15]:

the system of equations of equilibrium in the form of Lamé for soil massif displacements is obtained on the basis of generalization of Hooke's law taking into account heat and mass transfer and dependences of Lamé and Young modulus coefficients on salts solutions concentration and temperature

$$\begin{aligned}
& \mu_i(c_i, T_i) \Delta U_i + \left( \lambda_i(c_i, T_i) + \mu_i(c_i, T_i) \right) \frac{\partial \varepsilon_\theta^{(i)}}{\partial x} + \frac{\partial \lambda_i(c_i, T_i)}{\partial x} \varepsilon_\theta^{(i)} + 2 \frac{\partial \mu_i(c_i, T_i)}{\partial x} \frac{\partial U_i}{\partial x} + \frac{\partial \mu_i(c_i, T_i)}{\partial y} \left( \frac{\partial U_i}{\partial y} + \frac{\partial V_i}{\partial x} \right) + \\
& + \frac{\partial \mu_i(c_i, T_i)}{\partial z} \left( \frac{\partial U_i}{\partial z} + \frac{\partial W_i}{\partial x} \right) - \left( \left( 3 \frac{\partial \lambda_i(c_i, T_i)}{\partial x} + 2 \frac{\partial \mu_i(c_i, T_i)}{\partial x} \right) T_i + \left( 3 \lambda_i(c_i, T_i) + 2 \mu_i(c_i, T_i) \right) \frac{\partial T_i}{\partial x} \right) \alpha_T^{(i)} + X_i = 0, \\
& \mu_i(c_i, T_i) \Delta V_i + \left( \lambda_i(c_i, T_i) + \mu_i(c_i, T_i) \right) \frac{\partial \varepsilon_\theta^{(i)}}{\partial y} + \frac{\partial \lambda_i(c_i, T_i)}{\partial y} \varepsilon_\theta^{(i)} + 2 \frac{\partial \mu_i(c_i, T_i)}{\partial y} \frac{\partial V_i}{\partial y} + \frac{\partial \mu_i(c_i, T_i)}{\partial x} \left( \frac{\partial U_i}{\partial y} + \frac{\partial V_i}{\partial x} \right) + \\
& + \frac{\partial \mu_i(c_i, T_i)}{\partial z} \left( \frac{\partial V_i}{\partial z} + \frac{\partial W_i}{\partial y} \right) - \left( \left( 3 \frac{\partial \lambda_i(c_i, T_i)}{\partial y} + 2 \frac{\partial \mu_i(c_i, T_i)}{\partial y} \right) T_i + \left( 3 \lambda_i(c_i, T_i) + 2 \mu_i(c_i, T_i) \right) \frac{\partial T_i}{\partial y} \right) \alpha_T^{(i)} + Y_i = 0, \\
& \mu_i(c_i, T_i) \Delta W_i + \left( \lambda_i(c_i, T_i) + \mu_i(c_i, T_i) \right) \frac{\partial \varepsilon_\theta^{(i)}}{\partial z} + \frac{\partial \lambda_i(c_i, T_i)}{\partial z} \varepsilon_\theta^{(i)} + 2 \frac{\partial \mu_i(c_i, T_i)}{\partial z} \frac{\partial W_i}{\partial z} + \frac{\partial \mu_i(c_i, T_i)}{\partial x} \left( \frac{\partial U_i}{\partial z} + \frac{\partial W_i}{\partial x} \right) + \\
& + \frac{\partial \mu_i(c_i, T_i)}{\partial y} \left( \frac{\partial V_i}{\partial z} + \frac{\partial W_i}{\partial y} \right) - \left( \left( 3 \frac{\partial \lambda_i(c_i, T_i)}{\partial z} + 2 \frac{\partial \mu_i(c_i, T_i)}{\partial z} \right) T_i + \left( 3 \lambda_i(c_i, T_i) + 2 \mu_i(c_i, T_i) \right) \frac{\partial T_i}{\partial z} \right) \alpha_T^{(i)} + Z_i = 0,
\end{aligned} \tag{1}$$

where  $\mathbf{X} \in \Omega$ ,  $i = \overline{1, n}$  and the components of the mass forces in all layers of area  $\Omega$  are calculated by formulas

$$X_i = \begin{cases} \frac{dp_1^{(i)}}{dx}, & \mathbf{X} \in \Omega_i, \quad i = \overline{1, k}, \\ 0, & \mathbf{X} \in \Omega_{i^*}, \quad i = \overline{k+1, n}, \end{cases} \quad Y_i = \begin{cases} \frac{dp_2^{(i)}}{dy}, & \mathbf{X} \in \Omega_i, \quad i = \overline{1, k}, \\ 0, & \mathbf{X} \in \Omega_{i^*}, \quad i = \overline{k+1, n}, \end{cases} \quad Z_i = \begin{cases} \gamma_{zv}^{(i)} + \frac{dp_3^{(i)}}{dy}, & \mathbf{X} \in \Omega_i, \quad i = \overline{1, k}, \\ \gamma_{pr}^{(i^*)}, & \mathbf{X} \in \Omega_{i^*}, \quad i^* = \overline{k+1, n}. \end{cases} \tag{2}$$

Cauchy relations, expressing the dependencies of normal and tangential strains components on displacement components

$$\varepsilon_x^{(i)} = \frac{\partial U_i}{\partial x}, \quad \varepsilon_y^{(i)} = \frac{\partial V_i}{\partial y}, \quad \varepsilon_z^{(i)} = \frac{\partial W_i}{\partial z}, \quad \varepsilon_{xy}^{(i)} = \frac{1}{2} \left( \frac{\partial U_i}{\partial y} + \frac{\partial V_i}{\partial x} \right), \quad \varepsilon_{xz}^{(i)} = \frac{1}{2} \left( \frac{\partial U_i}{\partial z} + \frac{\partial W_i}{\partial x} \right), \quad \varepsilon_{yz}^{(i)} = \frac{1}{2} \left( \frac{\partial V_i}{\partial z} + \frac{\partial W_i}{\partial y} \right), \tag{3}$$

the normal and tangential stresses based on the generalized Hooke's law in inverse form and the law of parity of tangential stresses taking into account the dependences of Lamé coefficients on salt concentration and temperature

$$\begin{aligned}
\sigma_x^{(i)} &= \lambda_i(c_i, T_i) \varepsilon_\theta^{(i)} + 2 \mu_i(c_i, T_i) \varepsilon_x^{(i)} - \left( 3 \lambda_i(c_i, T_i) + 2 \mu_i(c_i, T_i) \right) \alpha_T^{(i)} \overline{T_i}, \\
\sigma_y^{(i)} &= \lambda_i(c_i, T_i) \varepsilon_\theta^{(i)} + 2 \mu_i(c_i, T_i) \varepsilon_y^{(i)} - \left( 3 \lambda_i(c_i, T_i) + 2 \mu_i(c_i, T_i) \right) \alpha_T^{(i)} \overline{T_i}, \\
\sigma_z^{(i)} &= \lambda_i(c_i, T_i) \varepsilon_\theta^{(i)} + 2 \mu_i(c_i, T_i) \varepsilon_z^{(i)} - \left( 3 \lambda_i(c_i, T_i) + 2 \mu_i(c_i, T_i) \right) \alpha_T^{(i)} \overline{T_i}, \\
\tau_{xy}^{(i)} &= 2 \mu_i(c_i, T_i) \varepsilon_{xy}^{(i)}, \quad \tau_{xz}^{(i)} = 2 \mu_i(c_i, T_i) \varepsilon_{xz}^{(i)}, \quad \tau_{yz}^{(i)} = 2 \mu_i(c_i, T_i) \varepsilon_{yz}^{(i)},
\end{aligned} \tag{4}$$

where  $\varepsilon_\theta^{(i)} = \varepsilon_x^{(i)} + \varepsilon_y^{(i)} + \varepsilon_z^{(i)}$ ,  $\mathbf{X} \in \Omega$ ,  $t > 0$ ,  $i = \overline{1, n}$ ,  $i^* = \overline{1, k}$ ,  $i^* = \overline{k+1, n}$ .

Boundary and conjugation conditions for displacements and stresses taking into account the thermal and chemical states of the soil massif are derived. Also the corresponding boundary value problem is supplemented by convective diffusion and convection mass and heat transfer equations and the generalized Darcy-Getsevanov law in the case of motion of salts solutions in the presence of a temperature gradient and the equation of continuity of liquid and solid phases with appropriate boundary and conjugation conditions for salts solutions concentrations, temperatures and piezometric heads.

We used the following dependences of the Young's deformation modulus and Lamé coefficients for the solution of *KCl* salts and temperature [4] and the following dependences of filtration coefficient from filtering fluid concentration and temperature:

$$E(c, T) = (a_{18} \cdot c^2 + a_{17} \cdot c + a_{16}) \cdot T^2 + (a_{15} \cdot c^2 + a_{14} \cdot c + a_{13}) \cdot T + a_{12} \cdot c^2 + a_{11} \cdot c + a_{10},$$

where  $a_{18} = 1,179 \cdot 10^{-5}$ ,  $a_{17} = -7,755 \cdot 10^{-4}$ ,  $a_{16} = 0,024$ ,  $a_{15} = -1,713 \cdot 10^{-3}$ ,  $a_{14} = 0,138$ ,  $a_{13} = -17,539$ ,  $a_{12} = 0,198$ ,  $a_{11} = -30,741$ ,  $a_{10} = 6,546 \cdot 10^3$ ;

$$\lambda(c, T) = (a_{28} \cdot c^2 + a_{27} \cdot c + a_{26}) \cdot T^2 + (a_{25} \cdot c^2 + a_{24} \cdot c + a_{23}) \cdot T + a_{22} \cdot c^2 + a_{21} \cdot c + a_{20},$$

where  $a_{28} = 1,177 \cdot 10^{-5}$ ,  $a_{27} = -9,23 \cdot 10^{-4}$ ,  $a_{26} = 0,018$ ,  $a_{25} = -1,558 \cdot 10^{-3}$ ,  $a_{24} = 0,128$ ,  $a_{23} = -14,343$ ,  $a_{22} = 0,166$ ,  $a_{21} = -25,543$ ,  $a_{20} = 5,611 \cdot 10^3$ ;

$$\mu(c, T) = (a_{38} \cdot c^2 + a_{37} \cdot c + a_{36}) \cdot T^2 + (a_{35} \cdot c^2 + a_{34} \cdot c + a_{33}) \cdot T + a_{32} \cdot c^2 + a_{31} \cdot c + a_{30},$$

where  $a_{38} = 1,242 \cdot 10^{-5}$ ,  $a_{37} = -1,983 \cdot 10^{-3}$ ,  $a_{36} = 0,084$ ,  $a_{35} = -1,3 \cdot 10^{-3}$ ,  $a_{34} = 0,191$ ,  $a_{33} = -12,748$ ,  $a_{32} = 0,085$ ,  $a_{31} = -13,816$ ,  $a_{30} = 2,533 \cdot 10^3$ ;

$$k(c, T) = a_0 + a_1 c + a_2 c^2 + (a_3 + a_4 c + a_5 c^2) T + (a_6 + a_7 c + a_8 c^2) T^2,$$

where  $c$ , the meaning of filtering fluid concentration,  $\frac{g}{l}$ ;  $T$ , temperature, °C;  $a$ , coefficients of approximating function which are determined as

$a_0 = -0,028$ ,  $a_1 = 6,37 \cdot 10^{-4}$ ,  $a_2 = -6,329 \cdot 10^{-7}$ ,  $a_3 = 2,42 \cdot 10^{-3}$ ,  $a_4 = -4,241 \cdot 10^{-5}$ ,  $a_5 = 7,744 \cdot 10^{-8}$ ,  $a_6 = -2,306 \cdot 10^{-5}$ ,  $a_7 = 1,005 \cdot 10^{-6}$ ,  $a_8 = -4,307 \cdot 10^{-9}$ .

#### 4. Computer modeling and results of numerical experiments

The inverse method is chosen to solve the SSS problems of soil massif, according to which the displacements of points are found first, then strains are found on the basis of Cauchy relations, and stresses are found behind them with the help of Hooke's generalized law. The Gauss-Seidel method and the sweep method were used to numerical solution of the SSS problems (1)-(4) with the corresponding boundary and conjugation conditions and additional equations [1]. We used finite-difference method instead of finite element method [15] for example.

As an example, the spatial displacements, normal and tangential deformations and stresses in the soil mass, consisting of three sub-areas (clay water saturated, sand water-saturated and soil in the natural state (dry)) in the region  $\Omega = \{X = (x, y, z): 0 \leq x \leq l_1, 0 \leq y \leq l_2, 0 \leq z \leq l_3\}$ .

The area  $\Omega$  was taken in the form of a rectangular parallelepiped of length  $l_1 = 10 m$ , thickness  $l_2 = 10 m$  and height  $l_3 = 10 m$ . The free surface is at the level  $l_3^{(2)} = 7 m$ , and under the area of clay soil has a height  $l_3^{(1)} = 3 m$  with the following initial data:

$$\begin{aligned} \tilde{T}_1(X, t) &= 30^0 C, & \tilde{T}_2(X, t) &= 15^0 C, & \tilde{H}_1(X) &= 10 m, & \tilde{H}_2(X) &= 1 m, & \tilde{C}_1(X, t) &= C_m = 350 \frac{g}{l}, \\ \tilde{C}_2(X, t) &= 8 \frac{g}{l}, & \tilde{C}_0(X, 0) &= 8 \frac{g}{l}, & \tilde{T}_0(X, 0) &= 5^0 C. \end{aligned}$$

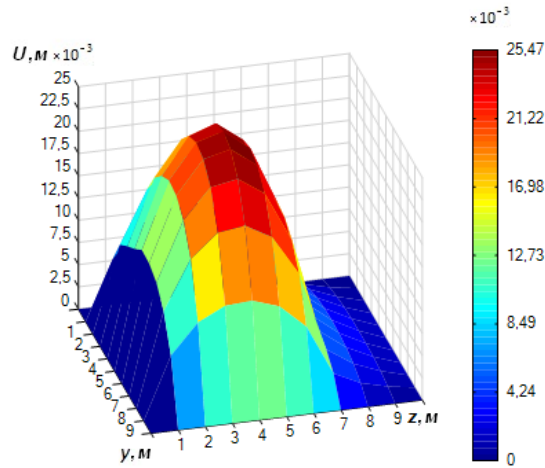


**Figure 2.** Distributions of displacements  $U(X)$  in cross section by plane  $yOz$  at  $x=5\text{ m}$

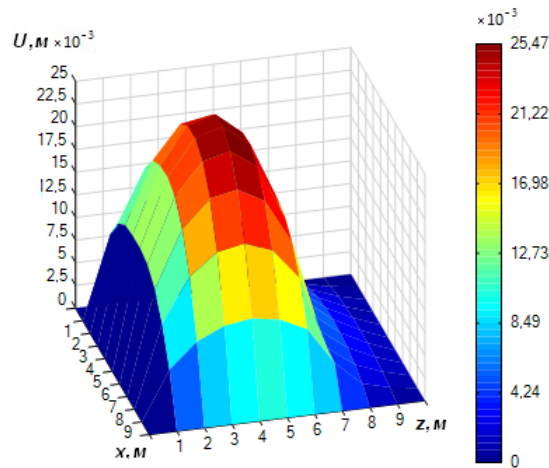


**Figure 3.** Distributions of displacements  $U(X)$  in cross section by plane  $xOz$  at  $y=5\text{ m}$

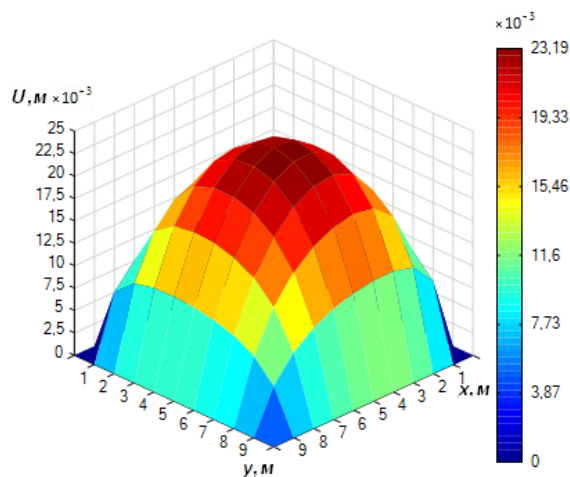


**Figure 4.** Distributions of displacements  $U(X)$  in cross section by plane  $xOy$  at  $z=5\text{ m}$

When analyzing the obtained results, it is shown that the largest values of spatial displacements are achieved in the subregions of water-saturated sandy soil. In the sub-areas of clay soil, the displacements are smaller than in sandy water-saturated ones due to the slow passage of pollution filtration and mass heat transfer.

## 5. Conclusions

The physical formulation of the problem of research of spatial deformation processes in a multilayer filtering soil massif is formulated in the article and its mathematical model is constructed. As a result of numerical solution and computer modeling of the required functions, displacements, normal and tangential deformations and stresses were obtained, which made it possible to estimate their values in different subregions of the soil massif.

## 6. References

- [1] Anatoliy Vlasyuk, Nataliia Zhukovska, Viktor Zhukovskyy, Rajab Hesham. Mathematical Modelling of Spatial Deformation Process of Soil Massif with Free Surface. *Advances in Intelligent Systems and Computing IV*. 2020. Vol. 1080. Pp. 107-120.
- [2] Hetnarski R. B. *Encyclopedia of thermal stresses*. Dordrecht: Springer Reference; 2014.
- [3] I. Kaliukh, O. Trofymchuk, and O. Lebid, "Numerical Solution of Two-Point Static Problems for Distributed Extended Systems by Means of the Nelder–Mead Method," *Cybernetics and Systems Analysis*, vol. 55, no. 4, pp. 616–624, 2019, doi: 10.1007/s10559-019-00170-3.
- [4] Kuzlo M. T. Investigation of the effect of the concentration of saline solutions on clutch forces in clay soils. *Hydrotechnical construction* 2013; 5:51–3.
- [5] Li, C., Xiu, Z., Ji, Y. et al. Analyzing the Deformation of Multilayered Saturated Sandy Soils under Large Building Foundation. *KSCE J Civ Eng* 23, 3764–3776 (2019).
- [6] Liqiang Cao, Dingli Zhang, Qian Fang. Semi-analytical prediction for tunnelling-induced ground movements in multi-layered clayey soils, *Tunnelling and Underground Space Technology*, 10.1016/j.tust.2020.103446, 102, (103446), (2020).
- [7] Sergienko I. V., Skopetskii V. V., Deineka V. S. *Mathematical Simulation and Investigation of Processes in Inhomogeneous Media*. Kiev: Naukova Dumka; 1991.
- [8] Sheng Wu, Dong-sheng Jeng. Numerical modeling of solute transport in deformable unsaturated layered soil. *Water Science and Engineering*. Volume 10. Issue 3. 2017. Pp. 184-196.
- [9] Skopetsky V. V., Bulavatskiy V. M. Mathematical Modeling of Dynamics of Consolidation Process on the Basis of System Approach. *J Automat Inf Scien* 2007; 39(8):11–9.
- [10] Vlasyuk A. P., Borowik B., Zhukovska, N.A., Zhukovskyy V. V., Karpinskyi V. Computer modelling of heat and mass transfer effect on the three-dimensional stressed-strained state of soil massif. 18th International Multidisciplinary Scientific Geoconference SGEM 2018 2018; 18(1.2):153–60.
- [11] Vlasyuk A.P., Zhukovska N.A., Zhukovskyy V.V. About Mathematical Modelling of Spatial Deformation Problem of Soil Massif with Free Surface. 2019 IEEE 14th International Conference on Computer Sciences and Information Technologies (CSIT). 2019. DOI: 10.1109/STC-CSIT.2019.8929794
- [12] XIU Zhan-guo, LI Chun, WANG Fei-li, QI Jia. Investigation on the Deformation Behavior of Multi-layered Soils Under a Large Foundation[J]. *Journal of Northeastern University Natural Science*, 2019, 40(12): 1779-1783.
- [13] Yamada Y., Ishihara K. Anisotropic Deformation Characteristics of Sand Under Three Dimensional Stress Conditions. *Soils and Foundations* 1979; 19(2):79–94.
- [14] Zhukovskyy, V., Sverstiuk, A., Sydoruk, B., Zhukovska, N., Sverstiuk, S. Analysis and Prediction of Humus Balance in Soils of Ukraine Using Informational Tools. *CEUR Workshop Proceedings* this link is disabled, 2022, 3309, pp. 259–270.
- [15] A. Safonyk, O. Prysiazhniuk, and I. Prysiazhniuk, "Modeling of the Processes of Heat and Mass Transfer in the Thin Tube Given the Conditions of Exchange with Surrounding Soil," 2019 IEEE 14th International Conference on Computer Sciences and Information Technologies (CSIT), , Lviv, Ukraine, 2019, pp. 100–103.